3D Printed Composite Model of Pelvic Osteochondroma and Nerve Roots

Olivia Fox
Westmead Hospital https://orcid.org/0000-0002-6299-7251
Andrew Kanawati (andrewkanawati@yahoo.com.au)
Westmead Hospital

Research Article

Keywords: 3D Print, Pelvic osteochondroma, Nerve roots, orthopaedic trauma, Surgical treatment, geometry, pelvic tumour

Posted Date: July 8th, 2021

DOI: https://doi.org/10.21203/rs.3.rs-656373/v1

Abstract

Purpose: 3D-printing has become increasingly utilized in the preoperative planning of clinical orthopaedics, orthopaedic trauma and other disciplines over the past decade. Surgical treatment of bone tumours within the pelvis is challenging due to the complex 3D bone structure geometry, as well as the proximity of vital structures such as blood vessels, nerve roots, sciatic and femoral nerves and the bladder and/or rectum.

Methods: We present the first case where a composite bone and nerve model of the lower lumbar spine, pelvis and accompanying nerve roots was created using 3D-printing. The bony pelvis and spine was created using CT, whereas the nerve roots were printed in an elastic material with the aid of MRI. 3D-printed model created an accurate reconstruction of the pelvic tumour and traversing nerves for preoperative planning and allowed for efficient and safe surgery. Pelvic tumour surgery is inherently dangerous due to the delicate nature of the surrounding anatomy.

Results: The composite model enabled the surgeon to very carefully navigate the anatomy with a focused resection and extreme care knowing the exact proximity of the L3 and L4 nerve roots.

Conclusion: The patient had complete resection of this tumour, no neurological complication and full resolution of his symptoms due to careful, preoperative planning with the use of the composite 3D model.

Introduction

3D printing has become increasingly utilized in the preoperative planning of clinical orthopaedics, orthopaedic trauma and other disciplines over the past decade. [1] Surgical treatment of bone tumours within the pelvis is challenging due to the complex 3D bone structure geometry, as well as the proximity of vital structures such as blood vessels, nerve roots, sciatic and femoral nerves and the bladder and/or rectum.

Reproducing the pre-operative plan as accurately as possible is crucial in pelvic tumour surgery, in order to achieve negative surgical margins and thus decrease the likelihood of local recurrence, and reduce the risk of damage to vital structures. [2–5] However, resecting significantly more tissue than planned, out of concern for leaving a positive margin, can compromise patient function and/or successful reconstruction. [3] Thus, accuracy in executing the pre-operative plan is crucial for safe surgical margins, preserving maximum bone stock, reducing surgical morbidity by allowing approach planning and increase understanding of nearby vital structures.

We present the first case where a composite bone and nerve model of the lower lumbar spine, pelvis and accompanying nerve roots was created using 3D-printing. The bony pelvis and spine was created using CT, whereas the nerve roots were printed in an elastic material with the aid of MRI. 3D-printed model created an accurate reconstruction of the pelvic tumour and traversing nerves for preoperative planning and allowed for efficient and safe surgery.

Case Report:

A 40 year-old male presented to our institution with a 20-year history of mild left-sided lower back and flank pain, secondary to an osteochondroma. His pain was activity related and was gradually increasing over two years. He occasionally complained of nocturnal symptoms.

Radiological imaging included serial CT and MRI of the lumbar spine (Fig. 1&2). The most recent scans revealed a lesion originating from the posteromedial aspect of the left iliac crest lesion, adjacent to and surrounding the left L5 transverse process. It had a stable appearance since the patient's puberty and had no aggressive radiological features of chondrosarcoma. The MRI revealed the proximity of the L3, L4 and L5 nerve roots as they exited the intervertebral foraminae and before they passed into the psoas muscle.

The patient was conservatively managed however after 5 months he represented with progression of his symptoms reporting depressive symptoms and cessation of work because of the pain. He started to complain of pain and numbness in his thigh and knee, due to L3 and L4 radiculopathies. He responded well to selective nerve root injections, however his symptoms recurred and operative management was decided upon.

3D-printing of the pelvis CT and lumbar spine MRI were used for preoperative planning (Fig. 3). The CT digital imaging and communication in medicine (DICOM) was imported into 3D Slicer version 4.10.2 (www.slicer.org). A region of interest was created around the left ilium, sacrum, L4 and L5 vertebrae, with a crop scale of 1.0 and isotropic spacing. The model was created by the 'grow from seeds' extension in the Segment Editor of 3D Slicer. Segmentation defects were corrected by modifying seeds and manual editing to ensure accuracy of the models. Closing (fill holes) and opening (remove extrusions) smoothing effects at a kernel size of 2mm were used to obtain a final model. The model was made hollow with a shell thickness of 2mm, and was exported as a standard tessellation language (STL) file. The MRI DICOM was imported into 3D Slicer. The axial T2 weighted sequences were used to identify the nerve roots. The 'draw tube' extension in the Segment Editor of 3D Slicer was used to trace the L3, L4 and L5 nerve roots using a 2mm radius. The nerve roots were combined into one model and exported as an STL file. The bone and nerve models were aligned to allow for closer assessment of the nerve roots relationship to the tumour. The L3 nerve was found to be traversing directly anterior to the lesion and actually form a groove on the anterior and cranial surface (Figs. 3 and 4). The L4 nerve root was found to be traversing directly medial to the lesion. The bone model STL file was imported into Formlabs Preform software (Version 3.0.2). Layer thickness was set to 0.1mm, supports were autogenerated and printed in Grey resin using a Formlabs Form 2 (Formlabs Inc. Somerville, MA) desktop 3D printer. The print time was 13 hours and 15 minutes, and print volume was 176 mls. The nerve root model STL file was imported into Formlabs Preform software. Layer thickness was set to 0.1mm, supports were autogenerated and printed in Elastic resin, using a Formlabs Form 2 desktop 3D printer. The print time was 3 hours and 45 minutes, and print volume was 18 mls.

The patient was positioned prone on a Jackson table after administration of a general anaesthetic. The tumour was approach via a posterior, longitudinal, paramedian incision (Wiltse approach). The posterior

aspect of the tumour was dissected in a subperiosteal manner. A bone scalpel (Misonix, Farmingdale, NY) was used to make one osteotomy at the base of the lesion, adjacent to the superomedial aspect of the ilium. The lesion was removed en-bloc. Complete resection of the lesion was confirmed by comparing the resected lesion to the 3D-printed model. Operative resection of the tumour took 58 mins, and was confirmed an osteochondroma on histology with negative surgical margins (Fig. 4). There were no intra- or postoperative complications, with complete resolution of symptoms at 2 weeks and 3 months postoperatively.

Discussion:

This case demonstrates a unique composite spine and pelvis model using a combination of 3D-printing of the exiting nerves from the MRI and the bony architecture from the CT scan. This created a benefit to the patient in explaining the operation and the risk of iatrogenic nerve injury, but also provided a guide for operative management.

Several procedures for improving surgical accuracy have been described, such as computer-assisted surgical navigation, robot-assisted surgery and use of 3D-printed patient-specific guides. [3; 6–9] Several studies have validated CT and MRI in the creation of accurate 3D-printed models, as well as the use of 3D Slicer in the creation of musculoskeletal segmentation. [10; 11] In a comparison of the 3D model and the cadaver pelvis, 3D printing resulted in accurate models suitable for preoperative workup. [12] 3D printing contributes to a better understanding of the surgical approach, reduction and fixation of fractures, especially in complex fractures such as acetabular fractures. [13–16] Furthermore, more accurate reduction and shorter operation times can be achieved. [17; 18] Additionally multiple cadaveric studies on pelvic tumours demonstrated more accurate osteotomies with 3D-printed patient-specific instruments compared to the standard manual technique. [19; 20]

Pelvic tumour surgery is inherently dangerous due to the delicate nature of the surrounding anatomy. The composite model enabled the surgeon to very carefully navigate the anatomy with a focused resection and extreme care knowing the exact proximity of the L3 and L4 nerve roots. The patient had complete resection of this tumour, no neurological complication and full resolution of his symptoms due to careful, preoperative planning with the use of the composite 3D model.

Declarations

No ethics approval was required for this case study and full patient consent was achieved, including consent for publication.

Availability of data and materials: Not applicable.

No funding or competing interests to declare.

Author's contributions: Olivia Fox was primarily responsible for the research, writing and publication of the case study. Andrew Kanawati was responsible for the care, CT and MRI 3D model construct and operative management of the patient.

Acknowledgements: Not applicable.

References

1. Bagaria V., S. Deshpande, D. Rasalkar. 2011. Use of rapid prototyping and three-dimensional reconstruction modeling in the management of complex fractures. European journal of Radiology. 80: 814 - 820.

2. Wirbel R., M. Schulte & W. Mutschler. 2001. Surgical treatment of pelvic sarcomas: oncologic and functional outcome. Clin Orthop Relat Res. 390: 190-205.

3. Khan F., A. Pearle, & C. Lightcap. 2013. Haptic robot-assisted surgery improves accuracy of wide resection of bone tumors: a pilot study. Clin Orthop Relat Res. 471: 851-859.

4. Bacci G., C. Forni, & A. Longhi. 2007. Local recurrence and local control of non-metastatic osteosarcoma of the extremities: a 27-year experience in a single institution. J Surg Oncol. 96: 118-123.

5. Nagarajan R., J. Neglia, & D. Clohisy. 2002. Limb salvage and amputation in survivors of pediatric lower-extremity bone tumors: what are the long-term implications? . J Clin Oncol. 20: 4493-4501.

6. Wong K. & S. Kumta. 2013. Computer-assisted tumor surgery in malignant bone tumors. . Clin Othop Relat Res. 471: 750-761.

7. Wong K., K. Sze, & I. Wong. 2016. Patient-specific instrument can achieve same accuracy with less resection time than navigation assistance in periacetabular pelvic tumor surgery: a cadaveric study. Int J Comput Assist Radiol Surg. 11: 307-316.

8. Jeys L., G. Matharu, & R. Nandra. 2013. Can computer navigation-assisted surgery reduce the risk of an intralesional margin and reduce the rate of local recurrence in patients with a tumour of the pelvis or sacrum? Bone Joint J. 95-B: 1417-1424.

9. Cartiaux O., L. Paul, & P. Docquier. 2010. Cartiaux O, Paul L, Docquier PL. Computer-assisted and robot-assisted technologies to improve bone-cutting accuracy when integrated with a freehand process using an oscillating saw. . J Bone Joint Surg Am. 92-A: 2076-2082.

10. Kanawati A, Fernandes RJR, Gee A, Urquhart J, Siddiqi F, Gurr K, Bailey C, Rasoulinejad P. 2020. Geometric and Volumetric Relationship Between Human Lumbar Vertebra and CT-based Models. Arcad Radiol. S1076-6332: 30332-9.

11. Kanawati A, Rodrigues Fernandes RJ, Gee A, Urquhart J, Bailey C, Rasoulinejad P. 2021. Geometric and volumetric relationship between human lumbar vertebrae and "Black-bone" MRI-based models. Int J Med Robot. 17: e2220.

12. Brouwers L., A. Teutelink, & F. van Tilborg. 2019. Validation study of 3D-printed anatomical models using 2 PLA printers for preoperative planning in trauma surgery, a human cadaver study. . Eur J Trauma Emerg Surg. 45: 1013-1020.

13. Hurson C., A. Tansey, & B. O'donnchadha. 2007. Rapid prototyping in the assessment, classification and preoperative planning of acetabular fractures. . Injury. 38: 1158-1162.

14. Mitsouras D., P. Liacouras, & Imanzadeh. 2015. Medical 3D printing for the radiologist. Radiographics. 35: 1965-1988.

15. Borrelli J., C. Goldfarb, & L. Catalano. 2002. Assessment of articular fragment displacement in acetabular fractures: a comparison of computerized tomography and plain radiographs. J Orthop Trauma. 16: 449-56.

16. Kim H., X. Liu & K. Noh. 2015. Use of a real-size 3D-printed model as a preoperative and intraoperative tool for minimally invasive plating of comminuted midshaft clavicle fractures. J Orthop Surg Res. 10: 91.

17. Zeng C., W. Xing, & Z. Wu. 2016. A combination of three-dimensional printing and computer-assisted virtual surgical procedure for preoperative planning of acetabular fracture reduction. Injury. 47: 2223-2227.

18. Chen X., J. Yuan, & C. Wang. 2010. Modular preoperative planning software for computer-aided oral implantology and the application of a novel stereolithographic template: a pilot study. Clin Implant Dent Relat Res. 12: 181-193.

19. García-Sevilla M., L. Mediavilla-Santos, & M. Ruiz-Alba. 2021. Patient-specific desktop 3D-printed guides for pelvic tumour resection surgery: a precision study on cadavers. Int J Comput Assist Radiol Surg. 16: 397-406.

20. Sallent A., M. Vicente, & M. Reverté. 2017. How 3D patient-specific instruments improve accuracy of pelvic bone tumour resection in a cadaveric study. Bone Joint Res. 6: 577-583.

Figures

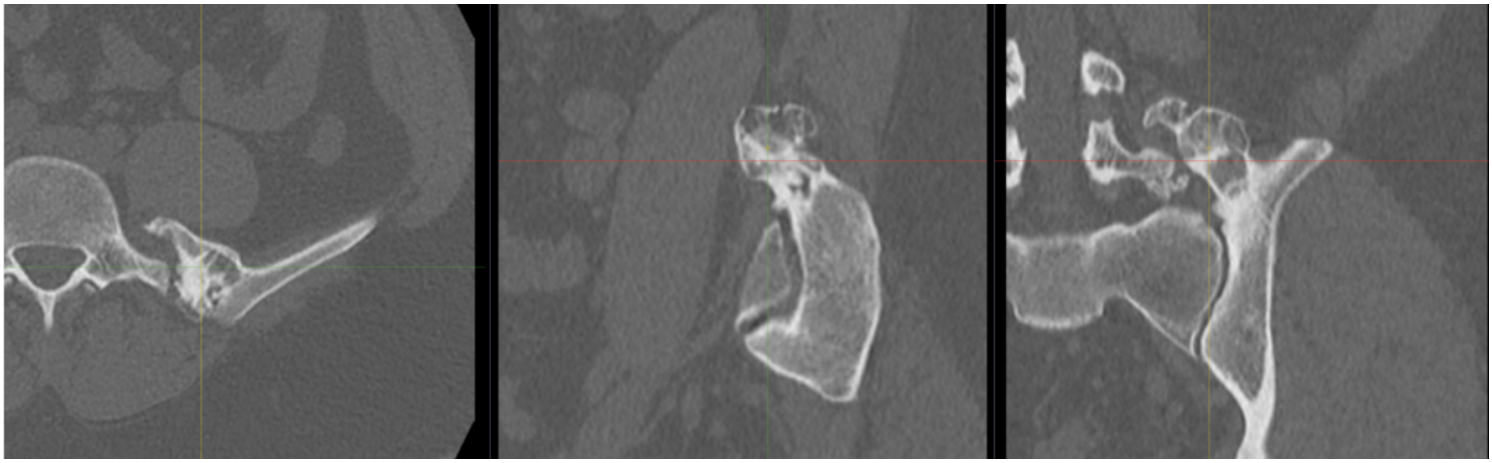

Figure 1

CT slices demonstrating the bony architecture of the osteochondroma.

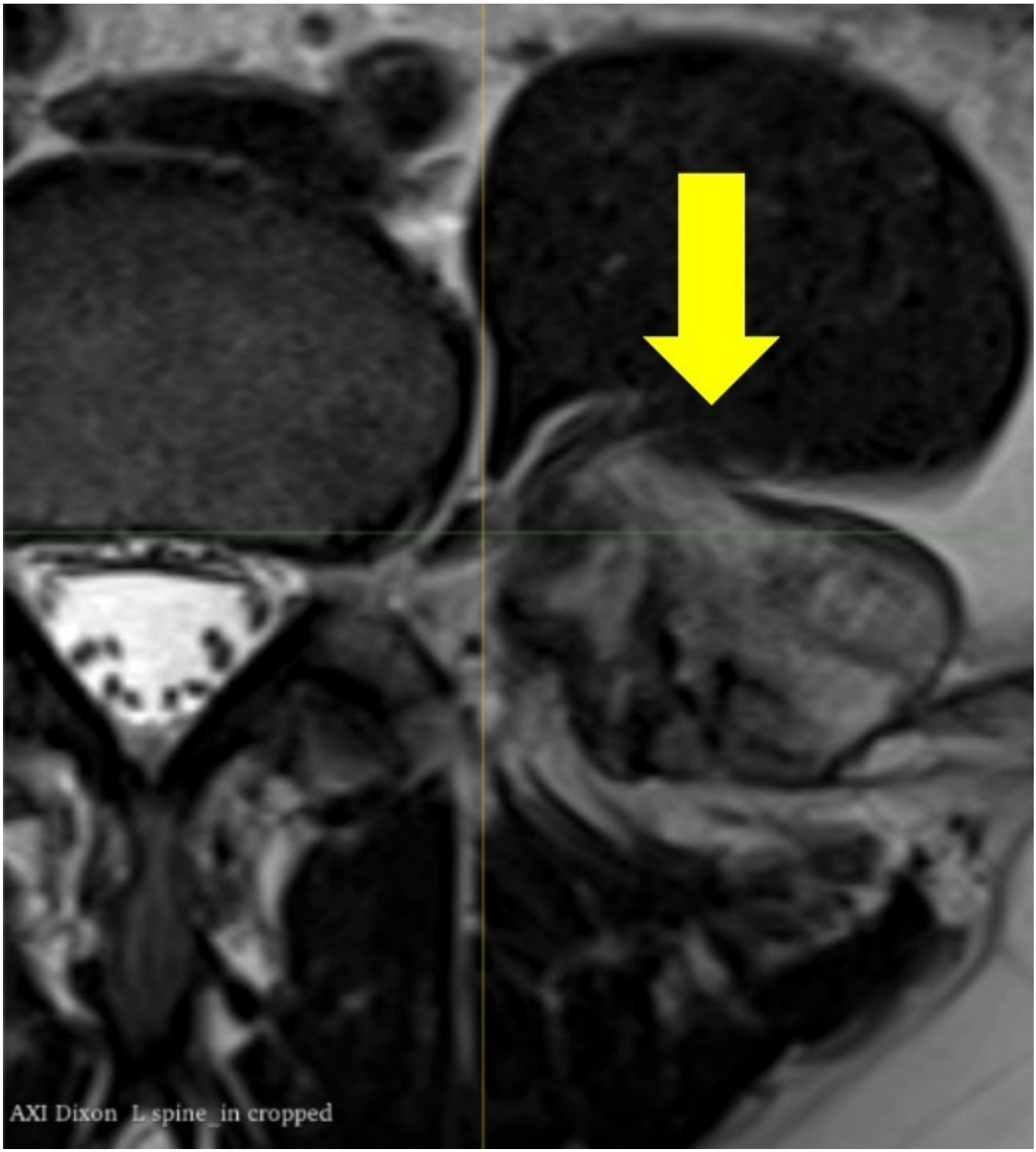

Figure 2

MRI demonstrating the L3 nerve root anterior tho the osteochondroma (arrow).

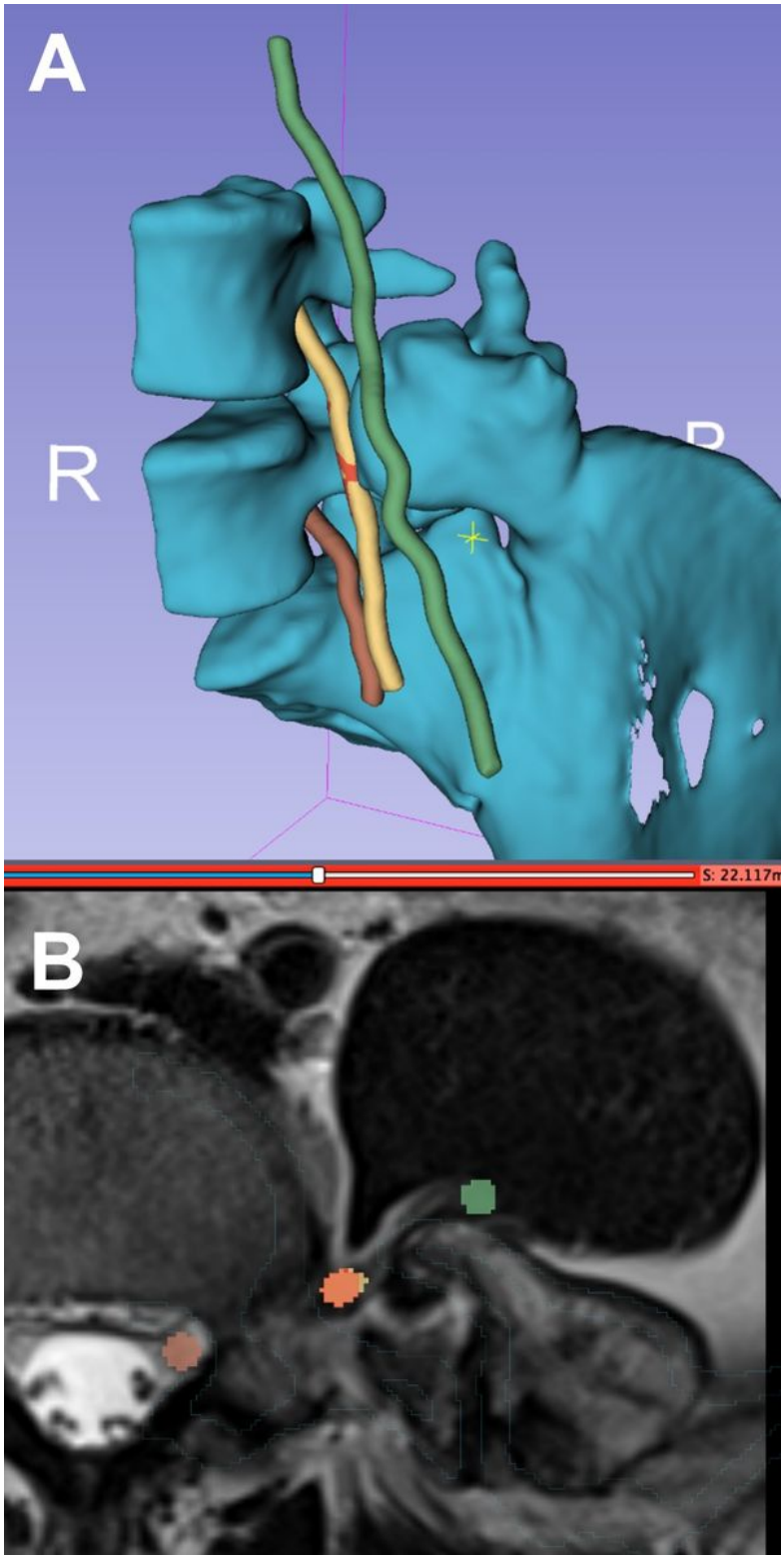

Figure 3

(A): Composite segmentation model of the left ilium osteochondroma based on CT data, and L3 – 5 nerve roots based on MRI data (B)

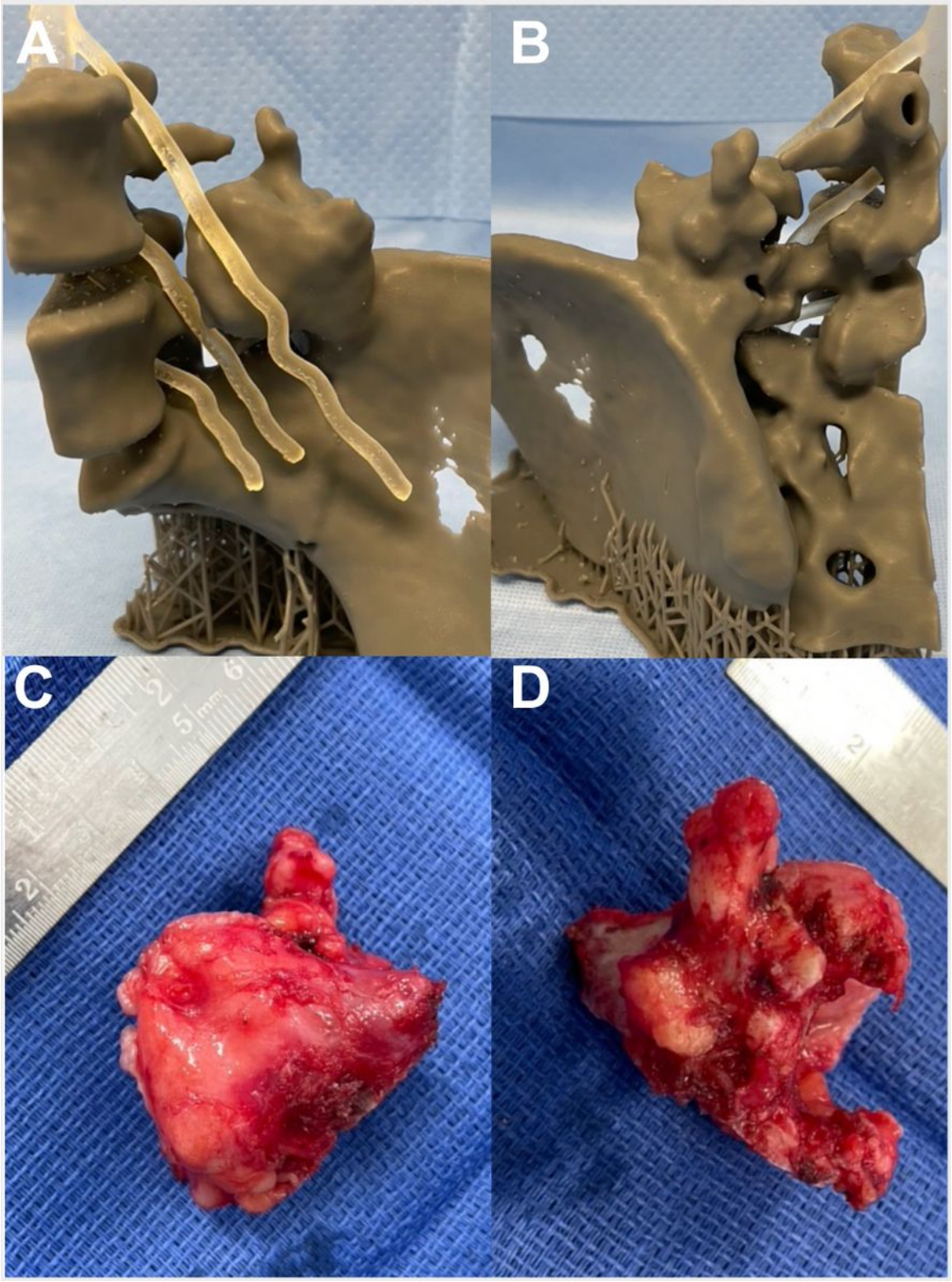

Figure 4

3D-printed model combining the CT and the MRI elements demonstrating the exact proximity of the nerve roots to the tumour. Anterior (A) and posterior (B) views. Corresponding anterior (C) and posterior (D) views of the excised osteochondroma.